Biochemistry and Biophysics Reports 22 (2020) 100766

Contents lists available at ScienceDirect

Biochemistry and Biophysics Reports

journal homepage: www.elsevier.com/locate/bbrep

Different effects of carbohydrate binding modules on the viscoelasticity of nanocellulose gels

Bart J.M. Rooijakkers[a], Suvi Arola[b], Rama Velagapudi[a], Markus B. Linder[a,*]

[a] Department of Bioproducts and Biosystems, School of Chemical Engineering, Aalto University, 02150, Espoo, Finland
[b] VTT, Technical Research Centre of Finland Ltd., High Performance Fiber Products, Tietotie 4E, 02150, Espoo, Finland

ARTICLE INFO

Keywords:
Cellulose nanofibril
Family 1 carbohydrate binding module
CBM
Gel
Rheology

ABSTRACT

Many cellulose degrading and modifying enzymes have distinct parts called carbohydrate binding modules (CBMs). The CBMs have been shown to increase the concentration of enzymes on the insoluble substrate and thereby enhance catalytic activity. It has been suggested that CBMs also have a role in disrupting or dispersing the insoluble cellulose substrate, but dispute remains and explicit evidence of such a mechanism is lacking. We produced the isolated CBMs from two major cellulases (Cel6A and Cel7A) from *Trichoderma reesei* as recombinant proteins in *Escherichia coli*. We then studied the viscoelastic properties of native unmodified cellulose nanofibrils (CNF) in combination with the highly purified CBMs to detect possible functional effects of the CBMs on the CNF. The two CBMs showed clearly different effects on the viscoelastic properties of CNF. The difference in effects is noteworthy, yet it was not possible to conclude for example disruptive effects. We discuss here the alternative explanations for viscoelastic effects on CNF caused by CBMs, including the effect of ionic cosolutes.

1. Introduction

Many lignocellulose-degrading enzymes contain a carbohydrate binding module (CBM) in addition to their catalytic domain to help guide the enzyme towards the substrate and bind to it. There are many different families of CBMs that vary in both structure and function, with affinity for different carbohydrates including cellulose, chitin and xylan [1]. Currently at least 86 different CBM families are known [2]. Of these, Family 1 (CBM1) is unique in that its members are found almost exclusively in fungal enzymes. They are relatively small domains of approximately 36 amino acids (~4 kDa), having two highly conserved disulfide bridges preserving a compact wedge-shaped structure [3–5]. Cellulose binding occurs through a combination of hydrogen bonding and π-stacking with three aromatic residues (most often Trp or Tyr) that are displayed on their cellulose-binding face [6–9].

Given their role in the enzymatic breakdown of various celluloses, CBM1 domains have been the focus of many research efforts [10–12]. CBM1s play a role in a wide variety of enzymes that fungi use to degrade cellulose, such as endoglucanases, cellobiose dehydrogenases, and lytic polysaccharide monooxygenases (LPMO). As these enzymes can be applied in biomass pretreatment, making surface modifications, or in the production of biofuels and other small-molecule chemicals, the interaction of CBM1s with different cellulose substrates is of great interest. Additionally, CBMs can be incorporated in genetically engineered proteins in order to create new protein-based materials such as cellulose-protein composites with specific and improved material properties [13–15]. Examples of CBM1s are found in the *Trichoderma reesei* exo-cellobiohydrolases Cel6A and Cel7A. Whereas these CBMs are highly similar, Cel6A-CBM1 features an additional disulfide bridge and Trp-Tyr-Tyr as binding residues, the Cel7A-CBM1 uses three Tyr residues (Fig. 1). It is interesting to note that CBM1 members often have a relatively low affinity towards cellulose, with a K_D in the order of magnitude of 1–10 μM depending on the substrate [16]. In comparison, members of other families that are found in bacterial enzymes often have much higher affinities. For example, the Family 3 CBM (CBM3) from the *Clostridium thermocellum* cellulosome scaffolding protein CipA, has a K_D of about 0.5 μM [17].

In several investigations, it has been suggested that CBMs can enhance the degradation of cellulose by acting as an auxiliary element. It was proposed that the binding of CBMs to cellulose materials could lead to the disruption of fibers, or disruption of interactions between fibrils, leading to increased access and activity of cellulases [21–23]. This hypothesis has been presented for various CBM-families, including examples specifically studying CBM1-members [24]. However, a detailed mechanism remains unclear and even alternative explanations cannot be ruled out, since preparations easily contain fractions of unknown activities that may act synergistically giving positive results by unrelated reasons. Most studies addressing the question of possible

* Corresponding author. Department of Bioproducts and Biosystems, School of Chemical Engineering, Aalto University, Box 16100, 00076-Aalto, Espoo, Finland.
E-mail address: markus.linder@aalto.fi (M.B. Linder).

https://doi.org/10.1016/j.bbrep.2020.100766
Received 27 January 2020; Received in revised form 19 February 2020; Accepted 7 April 2020

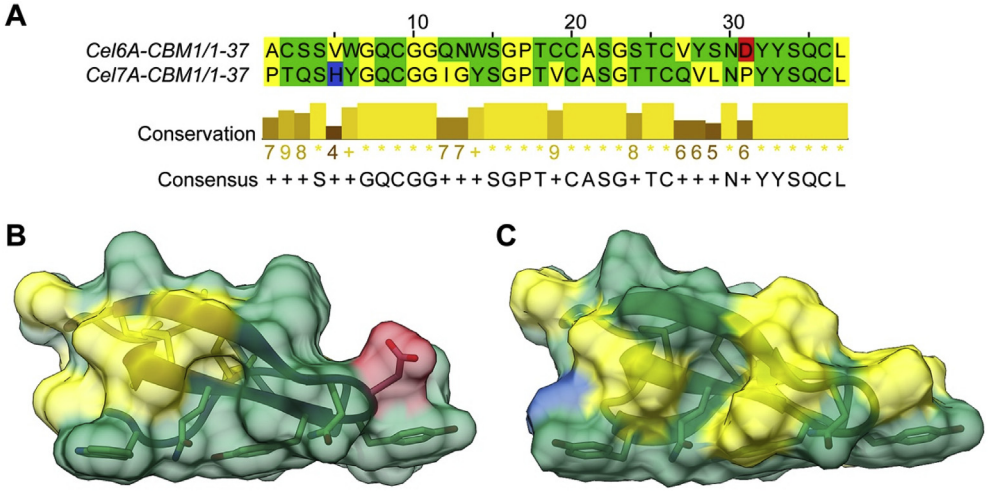

Fig. 1. A) Sequences of the Family 1 CBMs, Cel6A-CBM1 and Cel7A-CBM. Alignment made with MUSCLE and formatted with Jalview 2 [18,19]. B) Accessible surface of Cel6A-CBM1. C) Accessible surface of Cel7A-CBM1. On the accessible surfaces, the negatively charged Asp-residue in Cel6A-CBM1 is marked in red and the ionizable His-residue in Cel7A-CBM1 is marked in blue. No other ionizable side chains exist in the CBMs. Polar residues are marked in green, and hydrophobic in yellow, corresponding to the colors used in the sequences. The bottom parts of the structures have the aromatic residues that form the cellulose-binding face indicated. The structure of Cel7A-CBM has been solved by NMR [6](PDB ID: 1CBH), and Cel6A-CBM1 is a homology model based on 1CBH made with SWISS-MODEL [20]. (For interpretation of the references to color in this figure legend, the reader is referred to the Web version of this article.)

structural disruption of cellulose by CBMs take an approach of synergistic effects with enzyme action [21,24]. In some cases also x-ray diffraction [24] or observation of cellulose flocculation [23] have been used.

In this study we were interested to know how adding CBM proteins affect the rheological properties of native, unmodified cellulose nanofibrils (CNF) [25]. The CBMs were produced in *E. coli* as isolated domains, and were highly purified. CNF was produced from birch pulp and consists of elemental cellulose fibrils that are highly dispersed. They are thin, with a width about 2.5 to 3.5 nm, and have a high aspect ratio with a length in the range of several μm. CNFs are estimated to have a relatively low crystallinity of 8–12% [26]. Already at concentrations of 0.5–1% they form gels. These gels form by a percolating network of the CNF fibrils due to their relatively high stiffness and high aspect ratio. Furthermore, gel properties can be significantly affected by fibril contacts, bundling, and electrostatic interactions. In the non-modified type of CNF from birch pulp that were used here, there is also a dispersive effect enhanced by residual hemicellulose, xylan, that stay attached to the CNF during processing [27]. The gelling properties of CNF can be measured through viscoelasticity measurements using a rheometer. We chose to use CNF expecting that the highly dispersed and nanoscale character of CNF could yield new insight into the event of CBM binding to cellulose. In addition, CNF offers a balance of a well-defined material that still resembles the natural substrate of CBM1-containing enzymes.

2. Materials and methods

2.1. Construct design and plasmid preparation

Proteins were designed to have a N-terminal His-tag followed by a thrombin recognition sequence, a Smt3 cleavable carrier protein, and either Cel6A-CBM1 or Cel7A-CBM1 (full sequences are in the Supplementary Data). The His-tag and Smt3 were cleaved off by the protease ULP-1 [28,29]. DNA constructs were synthesized and subcloned into pET28a(+) expression vectors by GeneArt (Thermo Fisher). The resulting plasmids were verified by 1% agarose gel electrophoresis and sequencing (Eurofins).

The plasmid for producing *Clostridium thermocellum* CipA-CBM3 from the cellulosome scaffoldin protein CipA has been described in an earlier study [17]. The CipA-CBM3 belongs to Family 3.

2.2. Protein expression and purification

The plasmids for CBM1s were co-transformed into chemically competent BL21(DE3) *E. coli* together with a second plasmid pMJS205, carrying sequences for two proteins that actively aid in the proper formation of disulfide bridges in the cytoplasm. This procedure for *in vivo* disulfide formation is referred to as CyDisCo [30,31]. Individual colonies were picked and grown in pre-cultures in LB medium supplemented with kanamycin (50 mg/L) and chloramphenicol (35 mg/L), overnight at 37 °C. For production, MagicMedia expression medium (500 mL) (Thermo Fisher) was filled in Erlenmeyer flasks (2 L), supplemented with kanamycin (50 mg/L) and chloramphenicol (35 mg/L), inoculated with 1:10 of the pre-culture, and grown for 22–24 h at 30 °C, 230 rpm.

Cells were harvested by centrifugation (17000 × *g*, 4 °C, 10 min), and cell pellets were suspended in lysis buffer (20 mM NaH_2PO_4, 20 mM imidazole, 500 mM NaCl, 10 μg/mL DNAseI, 10 μg/mL $MgCl_2$, protease inhibitor cocktail (Sigma Aldrich) at 4 °C. After shaking for 30 min at 4 °C, the cell suspensions were further lysed by running them 2–3 times through an EmulsiFlex-C3 homogenizer (Avestin), after which the cell debris was removed by centrifugation (29000 × *g*, 4 °C, 30 min). The CBM1 proteins were purified from the supernatant using an ÄKTA Pure LC system and a HisTrap IMAC column (GE Healthcare). Subsequent purifications were done on a 2 mL Resource Reversed Phase Chromatography (RPC) (GE Healthcare) column by eluting with a gradient from water (MilliQ, Millipore) to 0–100% acetonitrile with 0.1% trifluoroacetic acid in both eluents. A final polishing step was performed on a RPC 214TP101015C4 column (Vydac) with the same eluents. Finally, the purified fractions were frozen and lyophilized. The resulting pure and salt-free protein powder was stored at room temperature in a desiccator.

The CipA-CBM3 protein was produced in the same way but without the CyDisCo plasmid and purified by HisTrap IMAC chromatography. The purified protein was desalted by two subsequent runs on a 10DG column (Bio-Rad) with water as the eluent.

The identity of CBMs was verified by SDS-PAGE (4–20%) with Coomassie Blue staining, RPC Ultra-high performance chromatography (UHPLC) (BioBasic 4 column, Vanquish, Thermo Fisher), and by directly injecting RPC UHPLC fractions into a Q-TOF 6350 mass spectrometer (Agilent). Protein concentrations were determined by measuring the absorption at 280 nm using a Varian Cary 50 UV-VIS spectrophotometer, corrected for background, and calculated using the extinction coefficient (Cel6A-CBM1 e = 15845; Cel7A-CBM1 e = 6210;

CipA-CBM3 $e = 35140$), based on protein sequence [32].

2.3. Binding assay

The CBM-cellulose binding assays were performed by mixing 100 μL CBM1 protein (50 mM TrisHCl pH 7 buffer) with 100 μL water (control) or 100 μL of 1 mg/mL CNF to a range of final protein concentrations of between 1 and 15 μM, followed by incubation at 23 °C for 1 h. The dispersions were then centrifuged at 23 °C for 2 min at 21000 × *g* to separate the supernatant (containing the non-bound CBM protein) for analysis. A Vanquish RPC UHPLC (Thermo Fisher) was used to analyze and quantify the non-bound proteins, by injecting 20 μL of the supernatant on a BioBasic 4RPC (Thermo Fisher) column and eluting by a gradient from water to 0–60% acetonitrile, both containing 0.1% trifluoroacetic acid.

2.4. Protein-CNF gel preparation

In order to prepare CNF-protein gels, appropriate amounts of CNF for rheology measurements were weighed, placed in separate tubes and water was added to a final concentration of 0.82% w/v. The CNF (in a 2 mL Eppendorf tube) was tip sonicated on ice for 2 min (2 s on/off cycles) with 20% amplitude (QSonica Q500). The CBMs were combined with the sonicated CNF and water at varying CBM concentrations and obtaining a final CNF concentration of 0.6% CNF. The dispersion was mixed for 5 s using a lab-bench vortex. Rheology experiments were started exactly 25 min after the sonication.

2.5. Rheology

Rheological measurements were carried out on an Anton Paar MCR302 strain-controlled rheometer at 23 °C (Peltier element + hood) using plate-plate geometry (diameter 25 mm). To counter evaporation effects, the Peltier hood and a filled water ring were attached. Viscoelastic properties were determined by performing small deformation oscillatory sweeps with 800 μL sample and a 1 mm gap. Measurements were done as follows, time sweep (frequency 0.1 Hz, strain 1%) for 20 min, frequency sweep (100–0.0159 Hz) at constant strain (1%), and strain sweep (0.01–100%) at a constant frequency (0.1 Hz). The time and frequency sweeps were performed at the linear visco-elastic region.

2.6. Step-Stress Creep recovery (SSCR)

For the SSCR, the same rheology setup was used, as well as the same sample preparation. A step-stress test was performed by measuring the strain during alternating steps of increasing steady levels of stress (creep, 2 min) and zero stress (recovery, 4 min), starting with a recovery step. The various stress steps were determined based on the previous stress sweeps and several test runs.

2.7. Atomic Force Microscopy (AFM)

In order to visualize the elementary fibrils of the CNF, a stock solution (1.69% w/w) was diluted to 0.15% (w/w) with water. The diluted sample was sonicated with a tip sonicator (QSonica Q500) for 10 min with 25% amplitude. The sonicated CNF solution was then centrifuged for 45 min at 10 000 × *g* after which a fraction of CNF was collected from the top of the sample by pipetting.

For imaging, 1x1 cm SiO_2 wafers were used as substrates. The wafers were thoroughly washed with ethanol and water. After washing, the wafers were dried under nitrogen gas and cleaned in an UV-ozone oven for 15 min. The wafers were coated with polyethylene imine (PEI) as an adhesive layer. The wafers were first submerged into 0.33% w/w solution of PEI for 15 min after which they were thoroughly washed. This involved first dipping into water several times, then keeping in water for 2 min, rinsing, and finally keeping in water for 5 min. The wafers were then dried under nitrogen gas. The CNF was diluted 1:10 and applied by spin-coating onto the wafers. Before applying cellulose, the wafer was wetted by with 50 μL water (3000 rpm, 20 s) and then 50 μL CNF sample was applied and spin-coated for 1 min (3000 rpm).

AFM imaging was done using a NanoTA AFM + instrument (Anasys Instruments, Bruker) with Mounted Standard Silicon Tapping Mode Probes with Al Reflex Coating (Applied NanoStructures). Images were recorded in tapping mode in air with scan rates of 0.4–0.6 Hz. The damping ratio was around 0.7–0.85. Images were flattened to remove possible tilts in the image data. Otherwise, no further processing of the images was done.

2.8. Cellulose Nanofiber (CNF) preparation

CNF was prepared from never-dried bleached Kraft birch pulp by disintegrating it with an ultra-fine friction grinder (Masuko Supermasscolloider) with rotation speed of 1500 rpm followed by ten passes through a high-pressure fluidizer (Microfluidics) [33]. The resulting samples with a solid content of 1.69% (w/v) were then stored at 4 °C.

3. Results and discussion

3.1. Atomic force microscopy

AFM confirmed the dispersed state of the CNF fibrils showing typical fibril diameters of 2.5–8 nm and lengths of fibrils in the range of several micrometers (Fig. 2). The results show that elementary fibrils as well as small bundles of fibrils were present.

3.2. Protein production and binding functionality

Our production strategy including solubility tags and the CyDisCo-system allowed for producing the CBM1s as isolated domains without linker sequences attached in a highly pure state and with disulfide bridges formed. The yield for purified protein was 10–15 mg/L.

To determine the binding functionality of the produced proteins, binding studies were performed on the pure CBM1 and studying their binding to CNF. In Fig. 3 the resulting binding isotherms of the proteins are shown. The binding parameters were comparable to ones previously published [16], with Cel7A-CBM1 having a higher affinity. The difference between the current and previous experiment is that here a different way of protein quantification was used, the way they were produced, and that here the CBMs lacked any residual linker regions.

3.3. Rheology

The viscoelastic properties of the cellulose-protein gels were analyzed extensively using rheology to investigate the effect of the CBMs on CNF. First, the linear viscoelastic region (LVR) was determined, after which time sweep, frequency sweep, and stress sweep measurements were performed. After initial screening, a concentration of 0.6% (w/v) CNF was chosen as the reference concentration to be used in all experiments. This was because this concentration represents the low end of the range where CNF forms a gel on its own, giving a soft gel that was highly responsive to changes in its chemical and structural environment. Initial experiments also showed that the CNF gels were highly responsive to the presence of salts such as NaCl. Even salts that co-purified with the proteins could result in effects on viscoelastic properties, which led us to prepare proteins with special care, including two separate and different RPC purification steps in highly purified water (conductivity 5 μS) and HPLC-grade solvents.

Fig. 4 displays an overview of the rheological properties of the CNF-CBM gels. Frequency sweeps (Fig. 4A) were performed for all samples between 100-0.0159 Hz at a constant 1% strain in LVR to obtain the

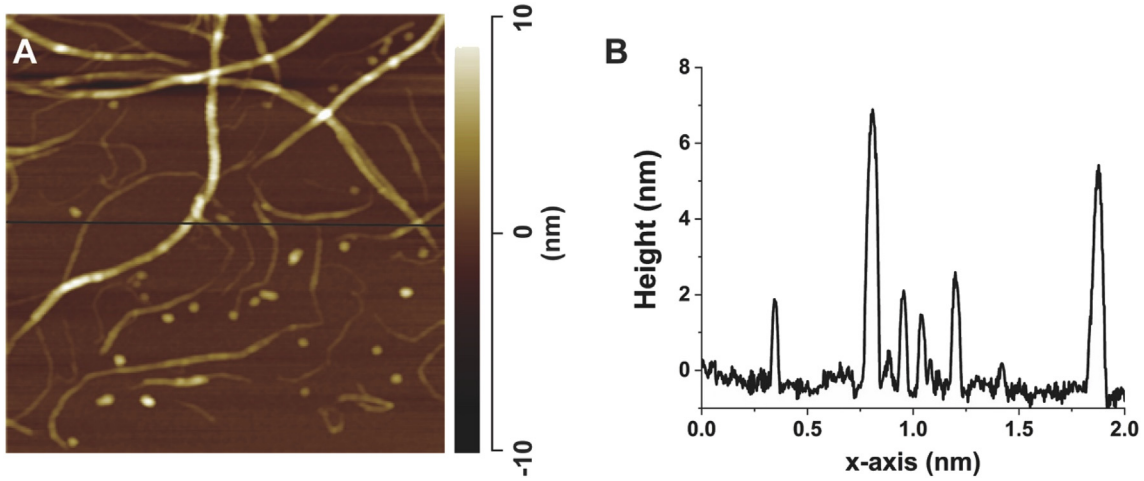

Fig. 2. AFM image of the CNF used in this study. A) An AFM image of the CNF fine fraction. The cross section in image B) shows the height of the elementary fibril (2.5–3.5 nm) and the length is estimated to be in the range of several μm.

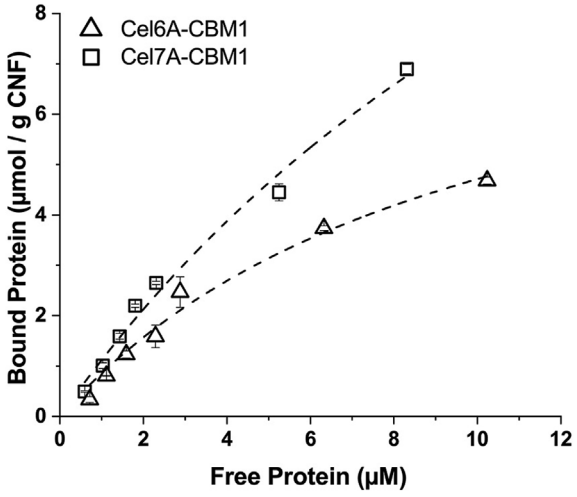

Fig. 3. Binding isotherms of Cel6A-CBM1 and Cel7A-CBM1 on CNF, displayed as against μmol of free protein plotted against μmol of bound CBM protein per gram of cellulose.

storage modulus (G') and loss modulus (G''). Stress sweeps were done at 0.1 Hz frequency in LVR (Fig. 4B). In Fig. 4C, the tan δ values (G''/G') from the frequency sweeps are shown. The protein concentrations in these measurements were set at 50 μM. The choice of this concentration was based on screening which showed that at this concentration, the differences between Cel6A-CBM1 and Cel7A-CBM1 were clear (Fig. 5A). At 50 μM a significant amount of protein was bound to the cellulose, and corresponding to about 50% saturation. The concentration dependency of NaCl on viscoelasticity was also measured (Fig. 5B).

A characteristic of CNF gels in general is their shear thinning tendency, i.e. to show lower viscosity at higher shear rates (Fig. 5C) when large deformation shear rate experiment is done. It can be seen that the starting viscosity at low shear rates is different between the samples and that the flow behavior of CNF with NaCl and CNF with Cel7A-CBM1 shows clear difference at low shear rates, i.e. the slope of the curves below shear rate 1 s^{-1} are steeper. However, all samples show a very similar thinning behavior during increased shear rate (rates above 1 s^{-1}). This suggests that at low shear rates the systems behave differently and more interactions are present in CNF samples with NaCl and Cel7A-CBM1 yet at higher shear rates, their general behavior under flow remained the same. What is interesting is that CNF with Cel6A-CBM1 does not differ from CNF alone and their flow behavior is very

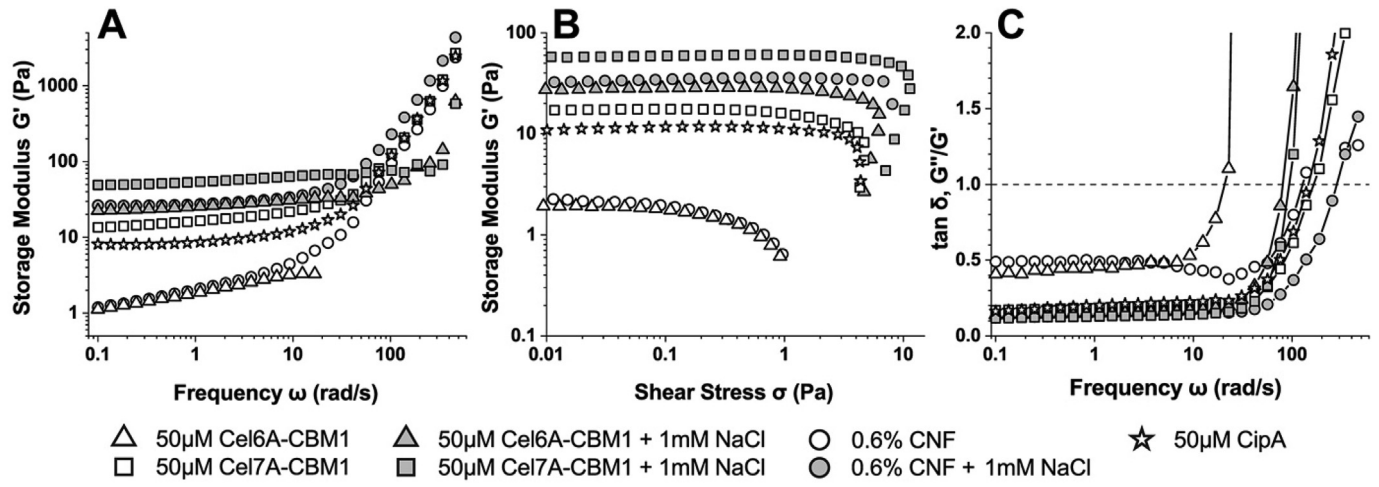

Fig. 4. Stress and frequency sweeps. A) Frequency sweeps and B) stress sweeps show that Cel6A-CBM1 and Cel7A-CBM1 affected the viscoelastic properties of CNF very differently. Cel6A-CBM1 had almost no effect, while Cel7A-CBM1 caused clear gelling. The samples containing CipA-CBM3 and only NaCl also showed increased gelling. C) All samples were gels as shown by the loss factor (tan δ). The gels collapsed at increased frequency, with the Cel6A-CBM1-containing sample being the weakest one. Open symbols represent samples in pure water and filled symbols show samples with NaCl added.

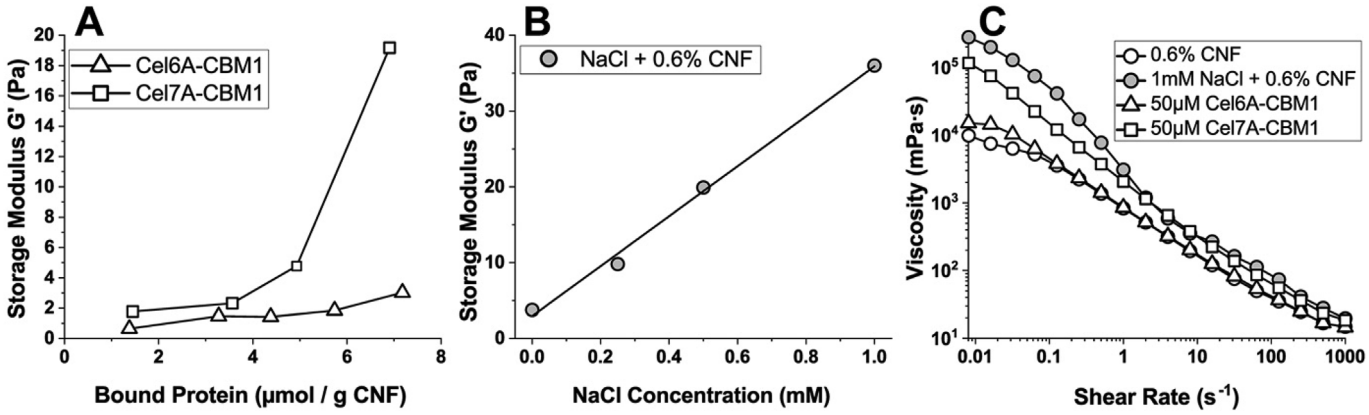

Fig. 5. Protein concentration dependency and shear tinning. A) Concentration dependence CBM1 on the G′ of CNF at 0.025 Pa stress. The x-axis shows how much CBM1 is bound to the cellulose. B) The dependence of NaCl concentration on the storage modulus of CNF at 0.025 Pa stress with a line showing a linear fit. C) Shear rate rheological measurements indicate shear thinning behavior of the CBM1-CNF gels.

similar regardless of the shear rate.

The data show that there are clear differences in the effects of Cel6A-CBM1 compared to Cel7A-CBM1 and CipA-CBM3 on the gelling of CNF. However, the effect of adding of NaCl to a final concentration of 1 mM gave in many respects a similar result as adding Cel7A-CBM1 or CipA-CBM3.

Between the different CBM1s, a very clear effect was seen in gelling and relative gel strength, so we continued to study gel properties by performing a creep recovery test, i.e. SSCR (Fig. 6). Under persistent load usually below the material's yield stress, polymer chains undergo stretching and re-orientation leading to changing in dimensions and even failure of the material (creep) [34]. Materials that can recover from creep i.e. materials that are resistant to creep are of great interest in long-term structural applications [35]. Thus, SSCR measurements give insight into the resilience of the material and its ability to recover from stress. These experiments are common in polymer research and have been applied for example to polymer composites routinely but have not been described extensively for CNF materials. In our SSCR, a constant stress was applied, and the effect on strain was measured. After applying constant stress during a fixed time, the stress was released and the effect on strain was recorded. The relaxation of the stress indicated the ability of the gel to recover, i.e. the elastic response of the material to applied load. Stress was then applied in repeated steps at increasingly higher values. When the applied stress surpassed the strength of the gel, the gel broke and no recovery was observed.

SSCR was performed for both the 0.6% CNF without additives and with either CBM1 proteins added. The CNF and CBM1 samples were also measured with 1 mM NaCl added. The plain 0.6% CNF as well as the Cel6A-CBM1 sample did not show recovery already after the first stress-step of 0.25 Pa. All samples containing NaCl and Cel7A-CBM1 showed much higher resistance to stress and recovery. Cel7A-CBM1 broke at 4 Pa, while the 1 mM NaCl containing samples at 8 Pa.

In summary, the work here explored the effects of two CBM1s on the viscoelastic properties of CNF. Since the percolating network of fibrils in CNF that results in bulk viscoelastic properties are dependent on fibril length and stiffness as well as interactions between fibrils [25], we speculated that binding or the previously suggested disruptive effects could be seen by rheological measurements. It is also clear that elemental fibrils are at least to some extent bundled in CNF, and any changes to such bundling is also expected to affect their effective length and stiffness, and the overall surface area of the solid fraction, thus affecting their viscoelastic properties. The sensitivity of viscoelastic properties for fibril interactions was previously used to understand the role of the hemicellulose component of CNF [27]. When interpreting results, it became very clear that care should be taken with sample preparation since the effect of NaCl addition shows that the gel network

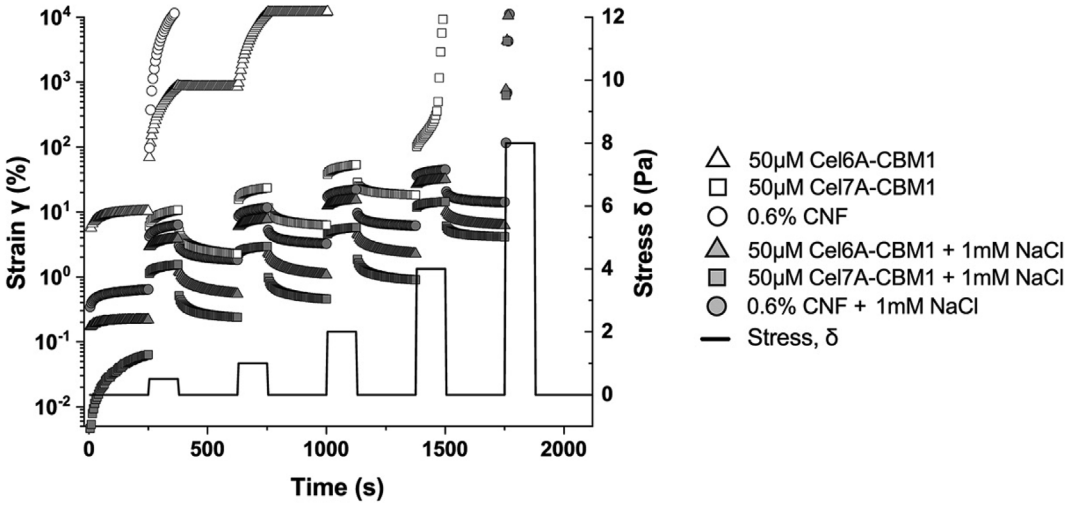

Fig. 6. Step-Stress Creep recovery rheology measurements of Cel6A-CBM1 and Cel7A-CBM1 with and without 1 mM NaCl, 0.6% CNF and CNF with 1 mM NaCl added. Creep is displayed as strain on the y-axis. The y-axis shows the steps of stress that were applied. The gel shows a recovery as reduced strain during the intervals of zero stress. When gels break, it is seen as a sharp increase in strain upon applying stress and showing no recovery during zero stress intervals. Stress was applied at increasing values in several steps of 1 min with intervals of 2 min with zero stress in between (i.e. recovery).

of connected CNF fibrils is highly sensitive to cosolutes in general [36]. The effect of salt has been noticed in particular for CNF preparations that have modifications to increase their negative charge, and thus their colloidal stability [37]. Although the CNF used in this work had a non-modified surface without any additionally introduced stabilizing charges, the CNF was highly sensitive to NaCl. This indicates that some excess charge can exist even in the non-modified version of CNF used here, perhaps as a part of the associated hemicellulose fraction [27,38]. The CNF itself was prepared using low ionic strength water, allowing efficient colloidal charge stabilization, and processing at relatively high cellulose concentrations [26,33].

It has been previously shown that creep recovery tests are useful when studying concentration dependent behavior of and interaction in CNF gel networks [39]. It was shown that an increase in mass fraction of carboxylated CNF led to an increase in stiffness of the hydrogels and the predominant response of the materials to applied stress was elastic, although all samples have some viscous character in the semi-dilute region. In our work, the viscous response was also seen in native CNF hydrogels with additives as was expected. The recovery of samples with Cel7A-CBM1 and NaCl showed more elasticity compared to CNF with Cel6A-CBM1 and CNF alone. Because of the high sensitivity of the CNF for different cosolutes, it is remarkable that the Cel6A-CBM1 had only a very small effect on the viscoelastic properties. It seems unlikely that Cel6A-CBM1 would have any fiber-disruptive properties, especially as relevant concentrations of at least 50% saturation of the CNF were investigated. On the other hand, effects of Cel7A-CBM1 are more difficult to understand, since there is a clear correlation between adding Cel7A-CBM1 and gel strength. For a fiber-disruptive function, this observation would be expected, since disruption could increase entanglement or release of hemicellulose could increase fibril interactions. Hence a disruptive effect cannot be excluded. If Cel7A-CBM1 did disperse fiber bundles, an increase in gel strength would be due to the ability of better dispersed fibrils to allow for more efficient percolation in the network. Attempts to study this by AFM did not show any clear evidence for disruption (data not shown), but it is expected that already sample preparation in AFM could possibly change the appearance of fibrils, making conclusions hard to draw by the technique.

An alternative explanation could be that Cel7A-CBM1 behaves in a salt-like way, i.e. a screening of charges present in the bound hemicellulose on CNF would result in less fibril repulsion and therefore to aggregation and increased gelling. This explanation would not support the suggestion that Cel7A-CBM1 could disrupt fibril bundling. However, when comparing the way NaCl and Cel7A-CBM1 affect in a concentration dependent manner (Fig. 5A and B), there is a difference. The NaCl affects in a linear fashion while Cel7A-CBM1 shows a response in a concave upward fashion. The effect of Cel7A-CBM1 seems therefore to be related to its binding. The non-linear effect of Cel7A-CBM1 may be related to some threshold being overcome only when a significant fraction of the maximal binding is achieved. The screening of charges by NaCl could be expected way linearly dependent on its concentration. We note that Cel7A-CBM1 has one His residue (Fig. 1). The pI of His is 6.0, which is the same as the pH of the system, meaning that Cel7A-CBM1 should not have a net charge. However, the pI of the His is altered due to a change of the local environment of the His residue, it may have a positive charge [40]. Comparing the Coulombic charges of proteins we note that Cel6A-CBM1 does have a single net negative charge, and on the other hand, CipA-CBM3 has a net of negative charged residues (Asp + Glu = 15, Arg + Lys = 11, pI = 5.01). Since the high-affinity CipA-CBM3 shows a strong gelling and Cel6A-CBM1 does not, it seems that no clear conclusions could be made based on simple considerations of charge.

4. Conclusions

We can conclude that Cel6A-CBM1and Cel7A-CBM1 affect fibril interactions differently in CNF gels. It seems unlikely that Cel6A-CBM1 has any fiber-disruptive properties, while Cel7A-CBM1 show gelling effects for which a fibril-modifying function cannot be excluded. An alternative explanation could be found in subtle electrostatic effects or other effects on CNF dispersion, but effects of NaCl and Cel7A-CBM1 on the CNF gels are not consistent, and are an argument against this explanation. A clear conclusion is that using rheology to study interactions is very complicated due to the extreme sensitivity of the system towards the presence of ions. Related to our finding that Cel6A-CBM1and Cel7A-CBM1 affect fibril interactions differently, it is interesting to note that we have previously found that there is a difference in the way in which Cel6A-CBM1 and Cel7A-CBM1 interact with cellulose [16]. Our present observations on the difference between the two CBMs can therefore also reflect differences in their function on their native cellulosic substrate. The exact nature of this difference however remains unclear.

Author statement

BR: Conceptualization; Data curation; Methodology; Investigation; Validation; Visualization; Writing - original draft; SA: Conceptualization; Data curation; Supervision; Investigation; Validation;Visualization; Writing - review & editing. RV: Conceptualization; Data curation; Methodology; Validation; Investigation;Visualization; ML: Conceptualization; Validation; Funding acquisition; Project administration; Resources; Supervision; Writing - review & editing.

Declaration of competing interest

The authors do not have any competing interests.

Acknowledgements

We thank Lloyd Ruddock (University of Oulu, Finland) for providing us with CyDisCo plasmids. A. Sesilja Aranko is thanked for her help with cloning of the Smt3 constructs and providing the ULP-1 protease. The research presented in this article was funded by The Academy of Finland, projects #259034 and #311608, and The Academy of Finland Flagship Programme FinnCERES under Projects #318890 and #318891. This work was carried out under The Academy of Finland's Centre of Excellence programme.

Transparency document

Transparency document related to this article can be found online at https://doi.org/10.1016/j.bbrep.2020.100766.

Appendix A. Supplementary data

Supplementary data to this article can be found online at https://doi.org/10.1016/j.bbrep.2020.100766.

References

[1] B. Henrissat, Cellulases and their interaction with cellulose, Cellulose 1 (1994) 169–196, https://doi.org/10.1007/BF00813506.
[2] V. Lombard, H. Golaconda Ramulu, E. Drula, P.M. Coutinho, B. Henrissat, The carbohydrate-active enzymes database (CAZy) in 2013, Nucleic Acids Res. 42 (2014) D490–D495, https://doi.org/10.1093/nar/gkt1178.
[3] B. Henrissat, A classification of glycosyl hydrolases based on amino acid sequence similarities, Biochem. J. 280 (1991).
[4] P. Tomme, R.A.J. Warren, R.C. Miller, D.G. Kilburn, N.R. Gilkes, Cellulose-Binding Domains: Classification and Properties, (1996), pp. 142–163, https://doi.org/10.1021/bk-1995-0618.ch010.
[5] A. Várnai, M.R. Mäkelä, D.T. Djajadi, J. Rahikainen, A. Hatakka, L. Viikari, Carbohydrate-Binding Modules of Fungal Cellulases, (2014), pp. 103–165, https://doi.org/10.1016/B978-0-12-800260-5.00004-8.
[6] P.J. Kraulis, G.M. Clore, M. Nilges, T.A. Jones, G. Pettersson, J. Knowles, A.M. Gronenborn, J. Kraulis, G.M. Clore, M. Nilges, T.A. Jones, G. Pettersson,

J. Knowles, A.M. Gronenborn, Determination of the three-dimensional solution structure of the C-terminal domain of cellobiohydrolase I from Trichoderma reesei. A study using nuclear magnetic resonance and hybrid distance geometry-dynamical simulated annealing, Biochemistry 28 (1989) 7241–7257, https://doi.org/10.1021/bi00444a016.

[7] J. Lehtiö, J. Sugiyama, M. Gustavsson, L. Fransson, M. Linder, T.T. Teeri, The binding specificity and affinity determinants of family 1 and family 3 cellulose binding modules, Proc. Natl. Acad. Sci. U. S. A 100 (2003) 484–9 http://www.pubmedcentral.nih.gov/articlerender.fcgi?artid=141021&tool=pmcentrez&rendertype=abstract.

[8] M. Linder, M.-L. Mattinen, M. Kontteli, G. Lindeberg, J. Ståhlberg, T. Drakenberg, T. Reinikainen, Gör Pettersson, A. Annila, Identification of functionally important amino acids in the cellulose-binding domain of Trichoderma reesei cellobiohydrolase I, Protein Sci. 4 (1995) 1056–1064, https://doi.org/10.1002/pro.5560040604.

[9] M.-L. Mattinen, M. Kontteli, J. Kerovuo, M. Linder, A. Annila, G. Lindeberg, T. Reinikainen, T. Drakenberg, Three-dimensional structures of three engineered cellulose-binding domains of cellobiohydrolase I from Trichoderma reesei, Protein Sci. 6 (1997).

[10] M.E. Himmel, S.-Y. Ding, D.K. Johnson, W.S. Adney, M.R. Nimlos, J.W. Brady, T.D. Foust, Biomass recalcitrance: engineering plants and enzymes for biofuels production, Science 315 (2007).

[11] D.B. Wilson, Cellulases and biofuels, Curr. Opin. Biotechnol. 20 (2009) 295–299, https://doi.org/10.1016/j.copbio.2009.05.007.

[12] S. Varjonen, P. Laaksonen, A. Paananen, H. Valo, H. Hähl, T. Laaksonen, M.B. Linder, Self-assembly of cellulose nanofibrils by genetically engineered fusion proteins, Soft Matter 7 (2011), https://doi.org/10.1039/c0sm01114b.

[13] P. Mohammadi, G. Beaune, B.T. Stokke, J.V.I. Timonen, M.B. Linder, Self-coacervation of a silk-like protein and its use as an adhesive for cellulosic materials, ACS Macro Lett. 7 (2018) 1120–1125, https://doi.org/10.1021/acsmacrolett.8b00527.

[14] P. Mohammadi, A.S. Aranko, C.P. Landowski, O. Ikkala, K. Jaudzems, W. Wagermaier, M.B. Linder, Biomimetic composites with enhanced toughening using silk inspired triblock proteins and aligned nanocellulose reinforcements, Sci. Adv. 5 (2019), https://doi.org/10.1126/sciadv.aaw2541 eaaw2541.

[15] P. Laaksonen, A. Walther, J.M. Malho, M. Kainlauri, O. Ikkala, M.B. Linder, Genetic engineering of biomimetic nanocomposites: diblock proteins, graphene, and nanofibrillated cellulose, Angew. Chem. Int. Ed. 50 (2011) 8688–8691, https://doi.org/10.1002/anie.201102973.

[16] S. Arola, M.B. Linder, Binding of cellulose binding modules reveal differences between cellulose substrates, Sci. Rep. 6 (2016) 35358, https://doi.org/10.1038/srep35358.

[17] S. Voutilainen, A. Paananen, M. Lille, M. Linder, Modular Protein Architectures for pH-dependent Interactions and Switchable Assembly of Nanocellulose, (2019), https://doi.org/10.26434/chemrxiv.8010872.v1.

[18] R.C. Edgar, MUSCLE: multiple sequence alignment with high accuracy and high throughput, Nucleic Acids Res. 32 (2004) 1792–1797, https://doi.org/10.1093/nar/gkh340.

[19] A.M. Waterhouse, J.B. Procter, D.M.A. Martin, M. Clamp, G.J. Barton, Jalview Version 2–a multiple sequence alignment editor and analysis workbench, Bioinformatics 25 (2009) 1189–1191, https://doi.org/10.1093/bioinformatics/btp033.

[20] M. Biasini, S. Bienert, A. Waterhouse, K. Arnold, G. Studer, T. Schmidt, F. Kiefer, T.G. Cassarino, M. Bertoni, L. Bordoli, T. Schwede, SWISS-MODEL: modelling protein tertiary and quaternary structure using evolutionary information, Nucleic Acids Res. 42 (2014) W252–W258, https://doi.org/10.1093/nar/gku340.

[21] N. Din, H.G. Damude, N.R. Gilkes, R.C. Miller, R.A.J. Warren, D.G. Kilburn, C1-C(x) revisited: intramolecular synergism in a cellulase, Proc. Natl. Acad. Sci. U. S. A 91 (1994) 11383–11387, https://doi.org/10.1073/pnas.91.24.11383.

[22] C. Hervé, A. Rogowski, A.W. Blake, S.E. Marcus, H.J. Gilbert, J.P. Knox, Carbohydrate-binding modules promote the enzymatic deconstruction of intact plant cell walls by targeting and proximity effects, Proc. Natl. Acad. Sci. Unit. States Am. 107 (2010) 15293–15298, https://doi.org/10.1073/pnas.1005732107.

[23] N.R. Gilkes, D.G. Kilburn, R.C. Miller, R.A.J. Warren, J. Sugiyama, H. Chanzy, B. Henrissat, Visualization of the adsorption of a bacterial endo-β-1,4-glucanase and its isolated cellulose-binding domain to crystalline cellulose, Int. J. Biol. Macromol. 15 (1993) 347–351.

[24] M. Hall, P. Bansal, J.H. Lee, M.J. Realff, A.S. Bommarius, Biological pretreatment of cellulose: enhancing enzymatic hydrolysis rate using cellulose-binding domains from cellulases, Bioresour. Technol. 102 (2011) 2910–2915, https://doi.org/10.1016/j.biortech.2010.11.010.

[25] E. Kontturi, P. Laaksonen, M.B. Linder, A.H. Nonappa, A.H. Gröschel, O.J. Rojas, O. Ikkala, Advanced materials through assembly of nanocelluloses, Adv. Mater. (2018) 1703779, https://doi.org/10.1002/adma.201703779.

[26] M. Pääkkö, M. Ankerfors, H. Kosonen, A. Nykänen, S. Ahola, M. Österberg, J. Ruokolainen, J. Laine, P.T. Larsson, O. Ikkala, T. Lindström, Enzymatic hydrolysis combined with mechanical shearing and high-pressure homogenization for nanoscale cellulose fibrils and strong gels, Biomacromolecules 8 (2007) 1934–1941 http://pubs.acs.org/doi/abs/10.1021/bm061215p.

[27] S. Arola, J.M. Malho, P. Laaksonen, M. Lille, M.B. Linder, The role of hemicellulose in nanofibrillated cellulose networks, Soft Matter 9 (2013) 1319 http://xlink.rsc.org/?DOI=c2sm26932e.

[28] M.P. Malakhov, M.R. Mattern, O.A. Malakhova, M. Drinker, S.D. Weeks, T.R. Butt, SUMO fusions and SUMO-specific protease for efficient expression and purification of proteins, J. Struct. Funct. Genom. 5 (2004) 75–86, https://doi.org/10.1023/B:JSFG.0000029237.70316.52.

[29] C.-D. Lee, H.-C. Sun, S.-M. Hu, C.-F. Chiu, A. Homhuan, S.-M. Liang, C.-H. Leng, T.-F. Wang, An improved SUMO fusion protein system for effective production of native proteins, Protein Sci. 17 (2008) 1241–1248, https://doi.org/10.1110/ps.035188.108.

[30] F. Hatahet, V.D. Nguyen, K.E.H. Salo, L.W. Ruddock, Disruption of reducing pathways is not essential for efficient disulfide bond formation in the cytoplasm of E. coli, Microb. Cell Factories 9 (2010) 67, https://doi.org/10.1186/1475-2859-9-67.

[31] A. Gaciarz, J. Veijola, Y. Uchida, M.J. Saaranen, C. Wang, S. Hörkkö, L.W. Ruddock, Systematic screening of soluble expression of antibody fragments in the cytoplasm of E. coli, Microb. Cell Factories 15 (2016) 22, https://doi.org/10.1186/s12934-016-0419-5.

[32] E. Gasteiger, C. Hoogland, A. Gattiker, S. Duvaud, M. Wilkins, R. Appel, A. Bairoch, Protein identification and analysis tools on the ExPASy server, in: J.M. Walker (Ed.), Proteomics Protoc. Handb. Humana Press, 2005, pp. 571–607.

[33] M. Österberg, J. Vartiainen, J. Lucenius, U. Hippi, J. Seppälä, R. Serimaa, J. Laine, A fast method to produce strong NFC films as a platform for barrier and functional materials, ACS Appl. Mater. Interfaces 5 (2013) 4640–4647, https://doi.org/10.1021/am401046x.

[34] W. Zhang, A. Joshi, Z. Wang, R.S. Kane, N. Koratkar, Creep mitigation in composites using carbon nanotube additives, Nanotechnology (2007), https://doi.org/10.1088/0957-4484/18/18/185703.

[35] Y. Jia, Z. Jiang, J. Peng, X. Gong, Z. Zhang, Resistance to time-dependent deformation of polystyrene/carbon nanotube composites under cyclic tension, Compos. Part A Appl. Sci. Manuf. (2012), https://doi.org/10.1016/j.compositesa.2012.04.011.

[36] H.O. Ono, Y.S. Himaya, K.S. Ato, T.H. Ongo, H spin – spin relaxation time of water and rheological properties of cellulose nanofiber dispersion, Transparent Cellulose Hydrogel (TCG) (2004) 36, https://doi.org/10.1295/polymj.36.684.

[37] K. Sim, J. Lee, H. Lee, Flocculation Behavior of Cellulose Nanofibrils under Different Salt Conditions and its Impact on Network Strength and Dewatering Ability, (2015), pp. 3689–3700, https://doi.org/10.1007/s10570-015-0784-y.

[38] H.V. Scheller, P. Ulvskov, Hemicelluloses, Annu. Rev. Plant Biol. 61 (2010) 263–289, https://doi.org/10.1146/annurev-arplant-042809-112315.

[39] L. Jowkarderis, T.G.M. Van De Ven, Rheology of semi-dilute suspensions of carboxylated cellulose nanofibrils, Carbohydr. Polym. 123 (2015) 416–423, https://doi.org/10.1016/j.carbpol.2015.01.067.

[40] M. Linder, T. Nevanen, T.T. Teeri, Design of a pH-dependent cellulose-binding domain, FEBS Lett. 447 (1999) 13–16.